Photovoltaic Solar Energy Conversion

Martin A. Green
Centre for Photovoltaic Devices and Systems
University of New South Wales
Sydney 2052 Australia

Received July 21, 1995

Over recent years, there has been marked recent improvements in the efficiency of energy conversion of photovoltaics, enhancing this technology's potential as a long term energy generation option. This paper describes the physics behind these improvements and outlines factors placing the upper bounds upon perfommance, suggesting paths towards increased efficiency in the future.

I. Introduction

Photovoltaics provide an elegant, non-polluting approach to providing future energy requirements, both in developed and less developed countries. To make a major impact, the cost of photovoltaic cells has to decrease while their energy conversion efficiency increases. Considerable recent progress has been made in both areas, although the present paper will concentrate on those relating to energy conversion efficiency.

Although photovoltaic research dates back to the work of Bequerel in 1839, the first cells of reasonable efficiency were reported in 1954 as a result of the development of silicon technology at Bell Laboratories[1]. These cells were about 6% efficient. Calculations of the upper limits to efficiency made at that time suggested figures of 20% efficiency for Si cells, with GaAs having a slightly higher efficiency potential of 23% [2]. Both technologies exceeded their respective efficiency "limits" in 1985. The highest performance figures are now 24.0% and 25.7% respectively[3,4].

This paper will discuss the physics behind these recent efficiency improvements and outline the scope for further efficiency improvement in the future.

II. Basic characteristics

A solar cell is basically a large area p-n junction diode designed so that light can be coupled into the bulk regions (Fig. 1). Illumination creates free carriers in the cell by exciting electrons from the valence band of the semiconductor to the conduction band. The presence of the p-n junction gives directionality to the flow of these photogenerated carriers. At the cell terminals, the normal rectifying diode characteristics are displaced down into the fourth quadrant by this photogenerated current (Fig. 2).

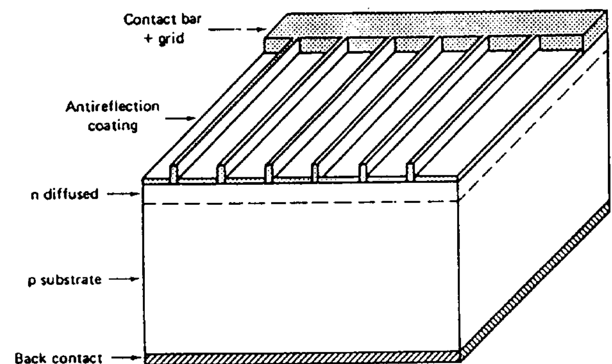

Figure 1. Solar cell schematic.

Important cell parameters are also defined in Fig. 2. These are the short circuit current (I_{SC}) (ideally equal to the photogenerated current) and the open circuit voltage (V_{OC}). The maximum power output is obtained when the cell is operating around the knee of the output curve and is less than the product V_{OC} I_{SC}. The fill factor (FF) is a third parameter which gives the actual power output as a fraction of this limiting value. The efficiency equals the product of the power output

$(FF^* \, V_{OC} \, ^* I_{SC})$ divided by the total power in the incident sunlight. Due to the exponential nature of the p-n junction characteristics, the fill factor is ideally a function of V_{OC} only at fixed temperature. Hence, cell efficiency is generally discussed in terms of I_{SC} and V_{OC}, with different cell features incorporated to individually optimize each of these two parameters.

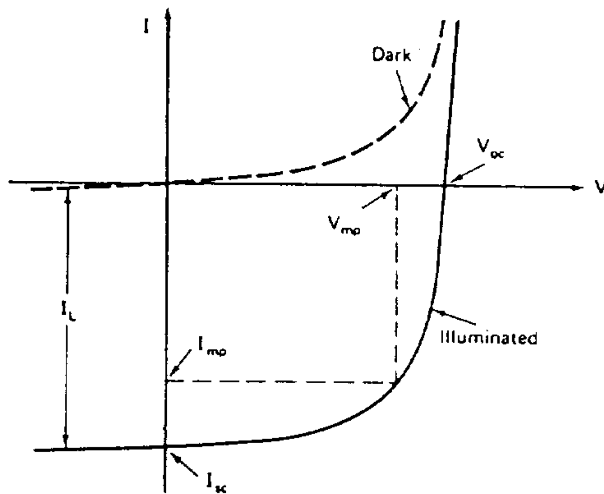

Figure 2. Output characteristics.

III. Present high efficiency cells

A diagram of a 24.0% efficient Si solar cell is shown in Fig. 3[3]. The most striking feature is the "inverted pyramids" on the top surface, incorporated to boost optical performance. Most light coming from above will be refracted into the cell at the point of initial incidence. With the pyramids, light reflected is reflected downwards and has another chance of coupling into the cell. Light coupled into the cell travels obliquely with shorter wavelengths strongly absorbed. Longer wavelengths reach the rear of the cell. The "dielectrically-displaced" metal reflector at the rear reflects about 97% of this light back obliquely across the cell. When it reaches the top surface, about haH is totally internally reflected by the pyramidal structure and is effectively "trapped" into the cell. These optical features contribute to the high I_{sc} of these cells.

V_{OC} is determined more by the electronic design of the cell. In the present case, the entire cell is enshrouded by a thin layer of thermally grown oxide. The $Si/Si0_2$ heterojunctions is one of the best characterized in semiconductor physics. In particular, oxide can be grown to maximize the quality of the resulting interface. Contact to the n- type region is made through parallel slots in this oxide. That to the p-type region is made through tiny holes in the oxide on the cell rear. The heavier doping in the contact areas on both top and rear surfaces minimizes the detrimental effects of high recombination rates occurring at the metal/Si interface. The cell is processed under conditions which maximize the "post-processing" quality of the Si, as reflected in the minority carrier lifetime (of the order of 1 ms for the present devices). These high values ensure that virtually every photogenerated carrier in the cell is "collected" (contributes to I_{sc}). The cell is designed with particular attention paid to minimizing parasitic series and shunt resistances which would degrade the cell fill factor.

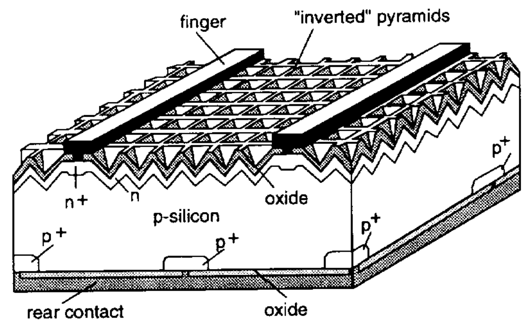

Figure 3. 24.0% efficient silicon solar cell.

Layer	Thickness	
MgF_2	0.12	COATING
ZnS	0.065	COATING
n - $GaInP_2$	0.03	CELL
n^+ - GaAs	0.1	CELL
p - GaAs	3.5	CELL
p - $GaInP_2$	0.1	CELL
p^+ - GaAs	substrate	

Figure 4. 25.7% GaAs cell.

GaAs is a direct bandgap semiconductor and also does not possess a thermal oxide of similar passivating properties. This produces design changes, as indicated in Fig. 4[4]. Due to the lack of passivating oxide, a thin layer of wider bandgap semiconductor (in this case $GaInP_2$) is grown epitaxially on the top surface of the GaAs to act as a weakly absorbing "window" layer. Compared to Si, the higher bandgap means that the GaAs cell responds to only the shorter wavelengths in the solar spectrum, producing a lower I_{SC} but a higher V_{OC}. The narrower bandwidth of the cell combined with the graded refractive index from the window layer to the cell bulk simplifies the optical design. A double layer antireflection coating combined with this graded index allows low reflection, reducing the benefits of pyramids. The more strongly absorbing direct bandgap material also reduces the benefits of the "light trapping" approach used in the Si cell. The "window" layer and the heavy doping of the substrate on which the cell is grown shield the high recombination regions at the metal/semiconductor interfaces. Again, attention is paid to maximizing the material quality in the cell bulk. Due to the direct bandgap, these tend to be lower than for Si with test structures similar to the devices of Fig. 4 showing lifetimes up to 14μs.

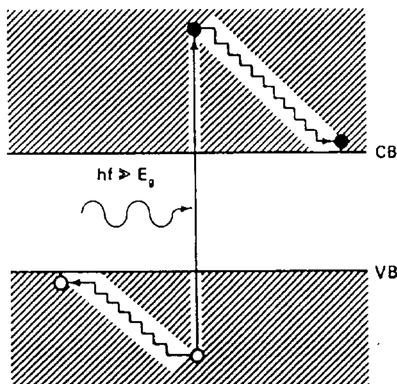

Figure 5. Major efficiency loss mechanism during electron-hole pair generation.

One major loss mechanism for both GaAs and Si cells is shown in Fig. 5. High energy photons create only one electron-hole pair within the semiconductor. The extra energy of the electron and hole above bandgap is quickly dissipated as heat (phonon emission). Each photon of energy larger than the bandgap therefore creates only one electron-hole pair with a final energy separation equal to the bandgap (very high energy photons can create more than one pair via impact ionization by the highly excited carriers, although a negligible effect in sunlight).

Layer	Thickness	
MgF_2	0.12	COATING
ZnS	0.065	
n - $AlInP_2$	0.04	TOP CELL
n - GaInP2	0.1	
p - GaInP2	0.8	
p+ - GaAs	0.02	TUNNEL DIODE
n+ - GaAs	0.02	
n - AlGaAs	0.2	BOTTOM CELL
n - GaAs	0.1	
p - GaAs	3.5	
p+ - GaAs	substrate	

Figure 6. Highly efficiency tandem cells.

Working with III-V compounds adds a new dimension to cell design, since the bandgap of the cell can be engineered. This allows cells of multiple bandgap to be built on the one substrate as in Fig. 6[5]. High energy photons are absorbed in the top cell while low energy photons pass through to the bottom cell. This allows the high energy photons to be converted at a higher voltage than otherwise possible. The heavily doped regions between the two cells provide a tunnelling junction which acts as an ohmic contact between them. Such cells have demonstrated efficiencies up to 29.5%. Although this approach could prove very important in the long term, it will not be addressed further (on the grounds that the performance of individual cells would still be constrained as below).

IV. Semi-empirical efficiency limits

The first approaches to calculating limits upon the conversion efficiency of photovoltaics were firmly based

on p-n junction device physics, together with a simplifying assumption about the useful photons in sunlight.

Fig. 7 shows the photon spectral distribution in two solar spectra. The extraterrestrial spectrum approximates that from a black body at 6,000K. However, scattering and absorption during passage through the atmosphere produces a more irregular terrestrial spectrum. To calculate the limit upon I_{SC}, a "threshold" approach is used. All photons in the sunlight of energy above the bandgap, E_G, are assumed to contribute one electron to the I_{SC}, with those of energy below the E_G giving zero contribution. Integrating the spectrum of Fig. 7 up to the corresponding cut-off wavelength and multiplying by the electronic charqe gives the upper limit to the cell current density.

From Fig. 2, the output current voltage characteristics of the cell are given by [6]:

$$I = I_0[\exp(qV/kT) - 1] - I_{SC}$$

where

$$I_0 = \frac{qD_n n_i^2}{L_n N_A} + \frac{qD_p n_i^2}{L_p N_D}$$

giving

$$V_{OC} = \frac{kT}{q} \ln\left(\frac{I_{SC}}{I_0} + 1\right)$$

These equations assume both p- and n-type regions are uniformly doped. $D_{n,p}$ and $L_{n,p}$ are the minority carrier diffusivity and diffusion length respectively, $N_{A,D}$ are the acceptor and donor doping levels in the respective regions, and kT/q is the "thermal voltage". (Minor correction terms are required when $L_{n,p}$ are larger than the device thickness[6]). The intrinsic carrier concentration, n_i, is given by:

$$n_i^2 = N_C N_V \exp(-E_G/kT)$$

where $N_{C,V}$ are the effective density of states of the two bands. Due to the strong dependence on E_G, n_i is the parameter varying most strongly between semiconductor materials.

To assign an upper limit to V_{OC}, most favourable values of the other semiconductor parameters are estimated. Fig. 8 shows the results calculated by Loferski in this way in 1955 [2]. As noted, present cells comfortably exceed these "limits", highlighting limitations of the semi-empirical approach.

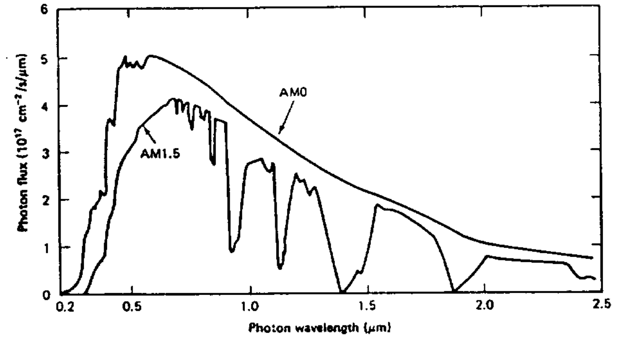

Figure 7. Photon flux in space (AM0) and terrestrial (AM1.5) sunlight.

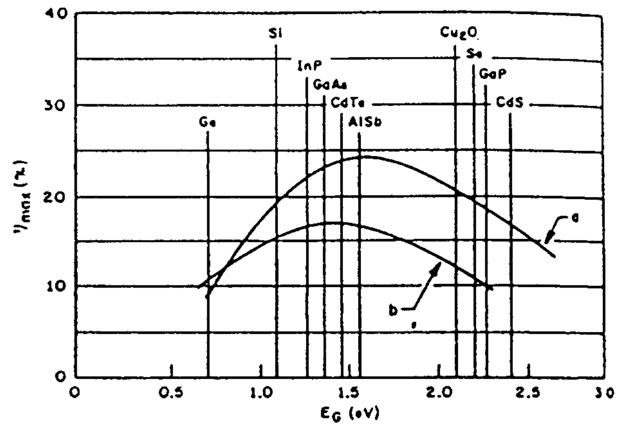

Figure 8. Semi-empirical efficiency limits [2].

V. Detailed balance limits

An important contribution to the topic of efficiency limits was made by Shockley and Quiesser[7]. These authors considered ideal material with carrier lifetimes limited by intrinsic radiative recombination. They noted that, in thermal equilibrium, the number of photons in the Planckian radiation emitted by the device of energy larger than the bandgap placed a lower bound on the number of recombination events in the cell.

They then argued that the intemal recombination rate increases as $\exp(qV/kT)$ where V is the cell's terminal voltage under illumination. This is quite reasonable, although not fully justified in the original paper. This can be proved if carrier mobilities are assumed infinite. It can also be shown to be the case for specific

designs which would work well as solar cells, including the multilayer cell discussed subsequently in Section IX. The upper bound on V_{OC} is obtained by equating the exponentially enhanced recombination rate to the total generation rate within the cell arising from illumination. The latter is calculated using the previous threshold approach. This approach projects higher efficiencies as might be expected. Peak efficiency of 32% is predicted for "black body" cells, with optimum bandgap Iying between those of Si and GaAs.

VI. Auger bounds

Green[8] has shown that the detailed balance limits for black body cells need not apply to thin cells with high levels of "light trapping", as could arise for a cell with a highly directional response[9]. Moreover, radiative recombination is a weak process in an indirect bandgap material such as Si. Other intrinsic processes, such as Auger recombination, were shown to impose lower intrinsic limits on the cell V_{OC}.

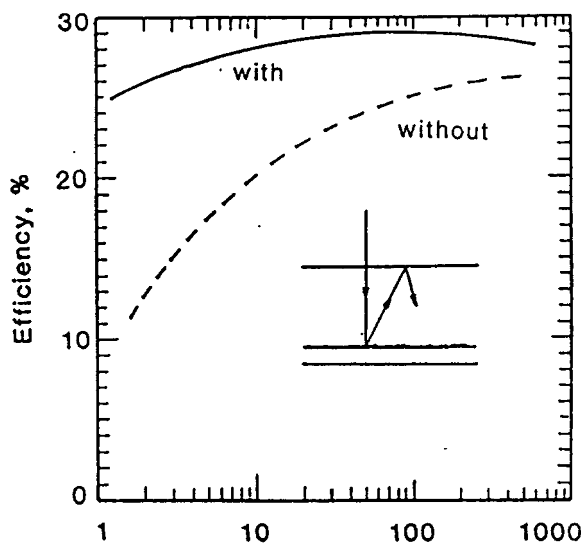

Figure 9. Auger limits on the efficiency of Si cells as a function of cell thickness (with and without light trapping).

The resulting theory shows that the limiting efficiency depends very much on the volume of the cell and the desired acceptance angle for solar radiation. Fig. 9 shows the results of these calculations for Si, suggesting a peak efficiency of just under 30% for a cell of about 100 μm thickness. An interesting result is that cells thinner than 10 μm can maintain similar efficiencies in contrast to conclusions if "light trapping" is excluded. This shows that high efficiency Si cells could be fabricated with much lower material costs than for present cells (about 400 μm thick). A recent extension to GaAs cells of this approach shows that light trapping is less important for these cells[10]. It does, however, show that the Auger recombination will limit GaAs cell performance under concentrated sunlight.

VII. Light trapping[11]

In calculating limits, it is important to know how effectively light can be trapped within the cell. Randomizing the light direction once into the cell causes effective trapping due to the small critical escape cone from Si due to its high refractive index, n. Such randomizing light schemes enhance the pathlength of weakly absorbed light by a factor of $4n^2$ (about 50 times for Si). Furthermore, the escape cone can be further restricted by limiting the acceptance angle of the cell for incoming light[9]. This enhances the pathlength of weakly absorbed light by a further factor of $(1/sin^2\theta)$ where θ is the half- angle of acceptance. If only the direct light from sunlight is to be used, as for systems based on concentrated sunlight, θ could be very small giving pathlength enhancements of up to 20 million, in principle!

VIII. Weak absorption

The enormous pathlength possible, in principle, using "light trapping" raises doubts about the threshold assumptions used to calculate limits to I_{SC}. For example, absorption of photons of energy near E_G in Si requires phonon participation to conserve energy and momentum. Phonon absorption makes it possible for Si cells to respond to photons with energy below E_G. Absorption involving two phonons is well documented for Si and extends the response of the experimental cell of Fig. 3 to energies 10% lower than the Si bandgap. Absorption with the help of three or more phonons could extend the response to even lower photon energies for a cell with sufficiently high light trapping.

These multi-quanta absorption processes suggest that the conventional threshold assumption is not tenable when high levels of light trapping are taken into account. As well as these multi-quanta processes, multi-

stage absorption processes could also enhance the absorption of sub-bandgap photons. Multi-quanta processes could also be multi-stage (e.g., Raman scattering followed by a phonon-assisted transition of the anti-Stokes photon). Multi-stage excitation through a midgap defect level by 2 photons is also feasible.

The question arises as to what actually will limit I_{SC}. The answer is that there are other intrinsic sub-bandgap absorption processes that do not result in electron hole pair creation. The most important of these at the wavelengths of interest is free carrier absorption. Since free carrier absorption increases strongly at longer wavelengths, it will eventually dominate the increasingly weak electron-hole pair production processes.

Preliminary work[11] has incorporated this reasoning into I_{SC} calculations, with results shown in Fig. 10. Shown is the I_{SC} bound for a Si cell, under the assumption of either infinite carrier mobilities or cell response to light from one direction only. Fig. 10 shows that, near short circuit, current output could be much higher than suggested by previous calculations due to weak absorption. However, due to increasing carrier densities as the cell voltage increases, the current near the cell operating point would be closer to the value given by the different threshold "approaches" indicated in Fig. 10.

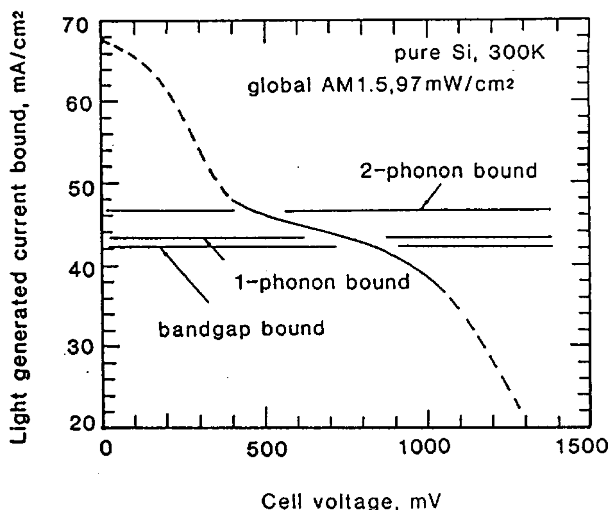

Figure 10. Calculated current bounds of a Si cell as a function of cell operating voltage.

IX. Multilayer cells

The parallel junction, multilayer cell of Fig. 11 has recently been proposed as a way of obtaining high performance from low quality silicon, such as deposited onto glass by chemical or physical vapour deposition. Since the junctions are in parallel, it does not possess the same advantages as the multijunction tandem cells, previously discussed.

Interestingly, it does allow the "infinite mobility" case to be approximated to any required degree of accuracy in experimental devices, by having each layer within the multilayer stack thin compared to a carrier diffusion length.

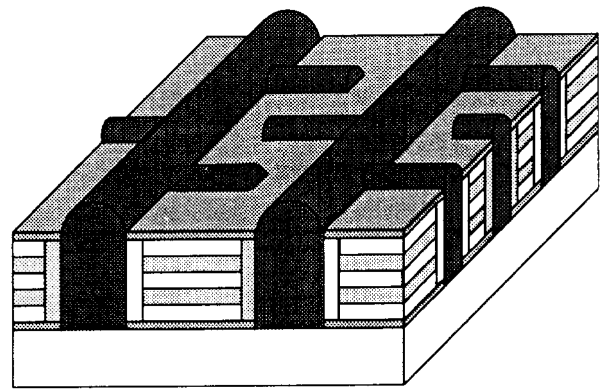

Figure 11. Parallel multijunction solar cell structure.

X. Conclusion

Despite marked improvements in solar cell performance over recent years, there remains scope for further large increases. It appears as if energy conversion efficiencies close to 30% will be demonstrated by single junction cells. Moreover, these high efficiencies may be attainable with low cell costs, since layers a few microns thick may be adequate. High efficiency (above 20%) in such thin layers could be obtained with optimized design of single junction cells as outlined in this paper or by the multiple cell "tandem" approach. High efficiency at low cost is required for photovoltaics to compete with conventional large scale electricity generators such as coal and nuclear plant.

Acknowledgements

I acknowledge contributions to this work by others within the Centre for Photovoltaic Devices and Systems, particularly Patrick Campbell, Mark Keevers and

Frans Saris. The work dealing with intrinsic silicon cell efficiency limits was funded by the Australian Research Council. The Centre for Photovoltaic Devices and Systems is funded by the Australian Research Council and by Pacific Power.

References

1. D. M. Chapin, C. Sler and G. L. Pearson, J. Appl. Phys., **25**, 676 (1954).
2. J. L. Loferski, J. Appl. Phys., **27**, 7770784 (1956).
3. J. Zhao, A. Wang, S. R. Wenham and M. A. Green, "24% Efficient Silicon Solar Cells", Conf. Record 1st World Conference for Photovoltaic Energy Conversion, December, 1994, unpublished.
4. J. M. Olson, S.R. Kurtz and A. Kibbler, "High Efficiency GaAs Solar Cells Using $GaInP_2$ Window Layers", Conf. Record, 21 st IEEE Photovoltaic Specialists Conference, May 1990, pp. 138-140.
5. K. A. Bertress, S. R. Kurtz, D.J. Friedman, A. E. Kibbler, C. Kramer and J. M. Olson, Appl. Phys. Lett. **65**, 989 (1994).
6. M. A. Green, *Solar Cells*, (Prentice-Hall, New Jersey, 1982).
7. W. Shockley and H. J. Queisser, Journal of Applied Physics **32**, 510 (1961).
8. M. A. Green, IEEE Trans. Electron Devices, **31**, 671 (1984).
9. P. Campbell and M. A. Green, IEEE Trans. Electron Devices, **33**, 234 (1986).
10. G. L. Araujo and A. Marti, IEEE Trans. Electron Devices, **37**, 1402 (1990).
11. M. A. Green, *Silicon Solar Cells: Advanced Principles and Practice*, (Bridge Printery, Sydney, 1995).
12. M. A. Green and S. R. Wenham, Appl. Phys. Lett., **65**, 2907 (1994).